Semiclassical vibration–rotation spectra of gaseous and physisorbed molecules

John E. Adams

Citation: The Journal of Chemical Physics **84**, 3589 (1986); doi: 10.1063/1.450194
View online: http://dx.doi.org/10.1063/1.450194
View Table of Contents: http://scitation.aip.org/content/aip/journal/jcp/84/7?ver=pdfcov
Published by the AIP Publishing

Semiclassical vibration–rotation spectra of gaseous and physisorbed molecules

John E. Adams
Department of Chemistry, University of Missouri–Columbia, Columbia, Missouri 65211

(Received 6 September 1985; accepted 22 November 1985)

A semiclassical spectral intensity method is applied to the calculation of vibration–rotation spectra both of isolated molecules and of molecules physically adsorbed on a solid surface. For the case of an isolated HCl molecule, we are able to generate discrete vibration–rotation spectral lines, the frequencies and integrated intensities of which agree well with the available literature values. Line shapes obtained for this case exhibit no evidence of broadening beyond the theoretical resolution of the calculation. Physisorption of the HCl on an Ar(111) surface leads, however, to a collapse of the *R*, *P* band structure at low rotational energies, with the free rotor dynamical limit being reached only at higher energies. The transition between dynamical regimes is associated with substantial line broadening and shifts in the line centers as well as with an increase in the desorption rate. A loss of rotational phase coherence appears to represent the principle line broadening mechanism in the present calculations.

I. INTRODUCTION

Vibration–rotation spectroscopy undoubtedly is one of the most powerful techniques available for the determination of molecular structures and bond energies. In the case of small gas-phase molecules, modern experimental methods that permit the accurate measurement of band intensities and theoretical advances that contribute to the interpretation of this spectral data have led to a fairly complete understanding of these simple systems.[1] Far less well characterized, however, are species in contact with condensed phases, since in these situations conventional normal mode analyses may be of little value. An important example of this type of system, one that is attracting considerable current interest is that of a molecule bound to a solid surface. While older work primarily involved transmission infrared spectroscopy of finely divided materials[2] (the substrate surface structure being very poorly understood in such cases), reliable data are more and more frequently being reported for molecules adsorbed on well-characterized single crystals. These results, particularly the ones deriving from infrared reflection absorption spectroscopy (IRAS), electron energy loss spectroscopy (EELS),[3] infrared emission spectroscopy,[4] multiple internal reflection infrared spectroscopy,[5] and similar sorts of measurements, are of a sufficiently high quality that even the shifts in spectral line positions that accompany changes in the surface coverage may be readily obtained, as may any temperature dependences of these shifts. In principle, it would seem possible to extract a wealth of information concerning adsorbate binding energies, binding geometries, molecular dynamics, and energy relaxation phenomena from these spectra, but actually doing so necessarily will be predicated upon the availability of convenient theoretical methods for simulating these spectra and thus for clarifying the relationship between the dynamics of adsorbed species and the observed spectra. We report here an attempt to provide just such a method which we feel will prove quite useful in elucidating many features of the experimental data for these systems.

The inspiration for the present study is found in a series of papers by Marcus and co-workers[6–8] dealing with the construction of molecular spectra on the basis of classical trajectory information. They have shown that for a number of assumed model potentials, one can calculate via a semiclassical spectral intensity method values for vibrational frequencies and intensities that agree quite well with the corresponding exact quantum results, not only for fundamentals but also for overtone and combination bands. In a related study, Stine and Noid[9] have calculated dipole matrix elements using this same technique for some diatomic molecules for which accurate interatomic potentials and dipole moment functions are available. They too showed through a comparison with quantum mechanical calculations that the semiclassical approach can provide a useful means for analyzing vibrational intensity data, with their prediction being that the real utility of the formalism probably will come in the description of polyatomic molecules, since for these species the quantum calculations become considerably more complex.

Several other examples of the use of classical trajectories in the calculation of spectra have also appeared in the literature in recent years. Most notable is the work of Berens and Wilson,[10] which is based on a purely classical (rather than semiclassical) molecular dynamics simulation that is corrected in an approximate way for quantum effects. From such a calculation involving many lengthy trajectories, one can obtain the envelope of the vibration–rotation absorption lines but not the discrete lines themselves. Of particular encouragement to us is the good agreement found between the calculated infrared band shape and the experimentally determined one for CO in various increasingly dense gaseous argon "solvents" and also in liquid-phase argon, inasmuch as it is the applicability of the formalism to the study of molecules in contact with condensed phases that constitutes our special interest here. On the other hand, Reimers and Watts[11] were not successful in applying this same version of the method to an investigation of the vibrational spectra of small clusters of water molecules, although it appears that

 0021-9606/86/073589-09$02.10

most of their difficulties stemmed from effects associated with the use of purely classical dynamics. Finally, the semiclassical theory has been adopted by Tully *et al.*[12] for a study of the widths of lines appearing in the vibrational spectrum of a hydrogen overlayer on a silicon surface. Not only were these workers able to calculate linewidths that could be compared favorably with the ones that they had measured, but also they determined that vibrational dephasing rather than relaxation is responsible for the line broadening at temperatures greater than, roughly, room temperature.

II. THEORY

The semiclassical spectral intensity method of Noid, Koszykowski, and Marcus[6,7] is based on the well-known result that the power spectrum of a dynamical variable is given by the Fourier transform of its corresponding autocorrelation function. In the case of absorption of infrared radiation, this prescription implies that the line shape function $I(\omega)$ can be written as

$$I(\omega) = (2\pi)^{-1}\int_{-\infty}^{+\infty} dt \,\langle \boldsymbol{\mu}(0)\cdot\boldsymbol{\mu}(t)\rangle e^{-i\omega t}, \tag{2.1}$$

where $\boldsymbol{\mu}(t)$ is the Heisenberg time-dependent dipole moment operator.[13] (This expression simply represents a recasting in the Heisenberg picture of the standard first-order time-dependent perturbation theory result.) The transition from quantum to classical mechanics is then made by replacing the above quantum operators by dipole moment functions, so that now one may construct the line shape simply by examining the time evolution of the dipole moment that is obtained from classical trajectories. In practice it is more convenient, however, to consider in lieu of Eq. (2.1) the following expression:

$$I(\omega) = (2\pi)^{-1}\lim_{T\to\infty} T^{-1}\left\langle \sum_{j=x,y,z}\left|\int_0^T dt\,\mu_j(t)e^{-i\omega t}\right|^2\right\rangle, \tag{2.2}$$

which, it has been shown, differs from the previous equation only by a term which vanishes in the long-time limit.[14] Note that the summation over Cartesian components here is required if rotational transitions are to be handled via this formalism.

We carry out the evaluation of Eq. (2.2) along the lines suggested by Wardlaw *et al.*,[8] namely by expanding $\mu(t)$ in a real Fourier series

$$\mu_j(t) = a_{0j}/2 + \sum_{k=1}^{N-1}[a_{kj}\cos(2\pi kt/T) + b_{kj}\sin(2\pi kt/T)], \tag{2.3}$$

where

$$a_{0j} = (2/T)\int_0^T dt\,\mu_j(t),$$

$$a_{kj} = (2/T)\int_0^T dt\,\mu_j(t)\cos(2\pi kt/T),$$

$$b_{kj} = (2/T)\int_0^T dt\,\mu_j(t)\sin(2\pi kt/T).$$

(These Fourier coefficients may be easily calculated using readily available fast Fourier transform methods.) Substitution of Eq. (2.3) into (2.2) leads then to the equation actually used here for the simulation of the absorption spectra

$$I(\omega) = (4\pi)^{-1}\lim_{T\to\infty}\left\langle \sum_j\sum_{k=1}^{N-1}(a_{kj}^2 + b_{kj}^2) \times\frac{\sin^2[(\omega_k-\omega)T/2]}{(\omega_k-\omega)^2T/2}\right\rangle, \tag{2.4}$$

$\omega_k \equiv 2\pi k/T$.

Since only for infinitely long trajectories does Eq. (2.4) reduce to a line spectrum (the theoretical resolution here is $\delta\omega = 2\pi/T$), one is really interested in the integrated intensity given by the area of the spectral peak, a quantity which can be written in the particularly simple form

$$\bar{I}(\omega_0) = (1/4)\left\langle \sum_j{\sum_k}' (a_{kj}^2 + b_{kj}^2)\right\rangle, \tag{2.5}$$

with the k summation involving only those terms for which ω_k is in the vicinity of the peak center, ω_0.

The semiclassical aspect of the method of Marcus and co-workers is now introduced into the theory through a choice of the initial conditions for trajectories that obeys a quantum–classical correspondence rule. An analytic intensity correspondence has previously been derived by Naccache[15] for the harmonic oscillator whereby one selects a classical action variable according to the following prescription: for the transition between states indexed by quantum numbers n_i and n_f, the appropriate action variable n_c is

$$n_c = [n_f!/n_i!]^{1/(n_f-n_i)} - (1/2). \tag{2.6}$$

Of particular interest here is the case $n_f - n_i = 1$ (i.e., dipole-allowed transitions), for which one obtains

$$n_c = n_i + \tfrac{1}{2},$$

a result that is equivalent to taking n_c to be the arithmetic average of the quantum numbers of the initial and final states. This simpler correspondence rule, namely

$$n_c = \tfrac{1}{2}(n_i + n_f), \tag{2.7}$$

in fact has been shown to yield intensities of transitions occurring in a nonresonant coupled oscillator system which are of comparable accuracy with those obtained using Eq. (2.6).[8] Thus, it appears likely that for most practical problems, mean action trajectories [Eq. (2.7)] will yield quite satisfactory absorption line shapes.

Note that a slight revision of the above general formalism will be required, though, if the calculations are to be useful in describing spectra of molecules adsorbed on metallic surfaces.[16] When an electric dipole is brought in the vicinity of such a surface, an image dipole is induced within the substrate at an equal distance from the surface plane. Orientation of the real dipole parallel to the surface leads to a corresponding alignment of its image *but* with the direction of the dipole reversed, and thus any change in the molecular dipole moment will be effectively cancelled by a simultaneous compensatory variation in the dipole moment of the image. On the other hand, a dipole lying perpendicular to the surface induces a collinear image dipole having an identical direction, with the net result being an enhancement (by roughly a factor of 2) of the absorption. Consequently, for such systems instead of including the total dipole moment of

the molecule in Eqs. (2.1)–(2.3), we should only consider that component of the dipole moment parallel to the surface normal.

III. SPECTRA OF ISOLATED MOLECULES: HCl

Although the semiclassical spectral intensity method has been successfully applied to the calculation of vibrational spectra, no determination of the discrete rotational fine structure of the vibrational band has appeared to date. We choose the simple diatomic $^1H^{35}Cl$ as our system for study on the basis of two important considerations: first, highly accurate potential energy and dipole moment functions are readily available, and second, the large rotation constant of this molecule[17] ($B_e \cong 10.6\ \text{cm}^{-1}$) will give rise to widely spaced and hence easily resolved rotational spectral lines.

The potential energy function assumed here for HCl is the Dunham oscillator potential described by Tipping and Ogilvie,[18] which is of the form

$$V(x_J, J) = hcB_e\gamma^{-2}(J)x_J^2\left(1 + \sum_{i=1}^{5} a_i(J)x_J^i\right),$$

where $x_J = (r - r_e)/r_e +$ "J corrections" (r = the HCl bond length, r_e = the equilibrium bond length (nonrotating molecule), and the correction terms account for the shift in the equilibrium position with rotation). The potential constants γ and $\{a_i\}$ are corrected for rotation of the molecule using the formulas of Ref. 18. On the basis of analytical matrix elements calculated using this potential as well as long-range *ab initio* results, Ogilvie, Rodwell, and Tipping[19] have determined a dipole moment function in a convenient Padé approximant form

$$\mu(x) = \mu_0(1 + x)^3/\left[1 + \sum_{i=1}^{7} e_i x^i\right],$$

with μ_0 being the equilibrium dipole moment (= 1.093 33 D), and the constants $\{e_i\}$ being an appropriate set of fitting parameters. These two functions were shown to lead to values of Herman–Wallis factors which agree satisfactorily with the experimentally derived quantities not only for the fundamental vibrational band but also for the first few overtones.

Initial vibrational and rotational energies for trajectories were chosen via the semiclassical prescription indicated in the previous section. Note, however, that a particular vibration–rotation transition in general will not be associated with a unique choice of the initial action variables. For example, the $R(0)$ spectral line corresponds to a change in quantum numbers (v, J) of (0,0) → (1,1), and so semiclassically one should take the action variables to have the values $(\frac{1}{2}, \frac{1}{2})$ in accordance with Eq. (2.6). On the other hand, the $P(1)$ line arising from the transition (0,1) → (1,0) should *also* derive from trajectories characterized by the initial action variables $(\frac{1}{2}, \frac{1}{2})$. Thus, for each choice of initial actions, one will obtain two spectral lines, one in the R branch and one in the P branch of the spectrum. Note also that, following the arguments of Marcus and co-workers,[6] only a single trajectory will be needed in order to calculate each R, P pair; a spectrum composed of m individual lines will require the generation of exactly $m/2$ quasiclassical trajectories.

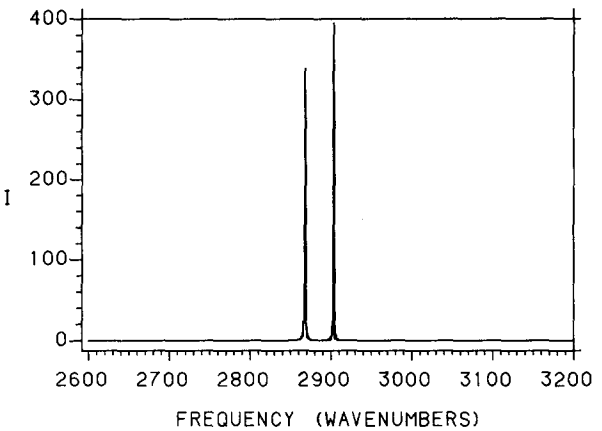

FIG. 1. $R(0)$ and $P(1)$ lines for a free $^1H^{35}Cl$ molecule. The units of the line shape function are $(D)^2$ s.

Having chosen a set of action variables, one may obtain initial coordinates and momenta for the two-atom system using standard techniques.[20] Each trajectory is then integrated for 24.573 ps with a time step of 1.0×10^{-4} ps, the values of the Cartesian components of the dipole moment being stored every 30 time steps. This procedure produces a grid of 8192 points per component, from which the fast Fourier transform routine constructs the 4096 Fourier coefficients per component that are subsequently combined to give 4096 individual intensities [Eq. (2.4)]. The theoretical spectral resolution here is 1.3576 cm^{-1}, and the maximum frequency obtainable is 5559.4 cm^{-1}.

In Fig. 1 we give the line shape function calculated on the base of one of these trajectories, specifically the trajectory that describes the (0,0) → (1,1) and (0,1) → (1,0) transitions [$R(0)$ and $P(1)$]. (A summary of the analysis of these peaks is found in Table I.) The calculated lines, as expected, are narrower than the theoretical resolution (FWHM $\approx$ 1 cm^{-1}), since it is unlikely that the small cou-

TABLE I. Spectral lines for free $^1H^{35}Cl$.

Line	v_c	J_c	Position $\tilde{\nu}(\text{cm}^{-1})$	$\bar{I}(D^2)$	$\bar{I}_{\text{ORT}}(D^2)$[a]
$R(0)$	1/2	1/2	2904 (2906)[b]	4.95×10^{-3}	4.94×10^{-3}
$P(1)$	1/2	1/2	2868 (2865)	5.16×10^{-3}	5.21×10^{-3}
$R(1)$	1/2	3/2	2925 (2926)	4.69×10^{-3}	4.81×10^{-3}
$P(2)$	1/2	3/2	2845 (2844)	5.26×10^{-3}	5.35×10^{-3}
$R(2)$	1/2	5/2	2944 (2945)	4.48×10^{-3}	4.68×10^{-3}
$P(3)$	1/2	5/2	2823 (2822)	5.25×10^{-3}	5.49×10^{-3}
$R(3)$	1/2	7/2	2963 (2963)	4.28×10^{-3}	4.55×10^{-3}
$P(4)$	1/2	7/2	2800 (2799)	5.29×10^{-3}	5.63×10^{-3}
$R(4)$	1/2	9/2	2981 (2981)	4.03×10^{-3}	4.43×10^{-3}
$P(5)$	1/2	9/2	2777 (2776)	5.30×10^{-3}	5.78×10^{-3}
$R(5)$	1/2	11/2	2999 (2998)	3.78×10^{-3}	4.31×10^{-3}
$P(6)$	1/2	11/2	2754 (2752)	5.21×10^{-3}	5.93×10^{-3}
$R(10)$	1/2	21/2	3080 (3072)	2.21×10^{-3}	3.75×10^{-3}
$P(11)$	1/2	21/2	2633 (2625)	3.96×10^{-3}	6.72×10^{-3}

[a] Intensities calculated using the results of Ogilvie, Rodwell, and Tipping, Ref. 19.

[b] The numbers in parentheses are the experimental values from Ref. 21.

pling between vibration and rotation in this molecule will lead to significant energy redistribution on the time scale of these trajectories. A good agreement is obtained here not only between the calculated peak positions and the experimental ones, but also between the integrated peak intensities $\bar{I}$ [from Eq. (2.5)] and the squares of the corresponding quantum matrix elements reported by Ogilvie, Rodwell, and Tipping.[19] We should point out here, though, that the intensity values which we report in Table I as being the results from the semiclassical spectral intensity method are in fact exactly twice as large as the values actually obtained from our calculations. Note that in order to use Eqs. (2.2), (2.4), and (2.5) correctly, one should average the calculated intensities over an ensemble of trajectories. However, in the case of pure vibration, it has been shown[6] (as we have mentioned above) that the result will be independent of the initial oscillator phase, regardless of whether the motion is quasiperiodic or ergodic; selecting different initial vibrational phases really just corresponds to starting the same trajectory at different points in its time evolution. In the case of rotation the situation is slightly different. For quasiperiodic motion the energetically accessible phase space is divided into two unconnected regions corresponding to different directions of rotation, such that a system rotating in a particular direction at time zero will never at a later time be found rotating in the opposite direction. Therefore, if the average over all of the allowed phase space is to be performed correctly, one must either combine the results from two trajectories that are identical except for the sense of the rotation or simply multiply the results from a single trajectory by a factor of 2 (the result from any single trajectory of course will be independent of the initial direction of rotation).

In Table I one will also find the results from trajectories associated with some of the other lines appearing in the fundamental band of $^1H^{35}Cl$. Even at the highest J_c values considered here, the calculated peak positions agree with the actual experimental values to 0.3% or better. The agreement with the quantum intensities derived from the expression given by Ogilvie, Rodwell, and Tipping[19] is also generally good; the semiclassical and quantum values differ by no more than about 10% except at the highest rotational energy. It is interesting to note, however, that the quantity $\bar{I}[P(J+1)]/\bar{I}[R(J)]$ for a given J, i.e., the ratio of the intensities of the two lines given by a single set of classical action variables, is nearly identical for the semiclassical and quantum intensities (the agreement is better than 1% for *all* J values, including $J=10$). None of the lines in the free-molecule spectra obtained here exhibit a broadening beyond that which would be expected from a consideration of the theoretical resolution.

IV. SPECTRA OF PHYSISORBED MOLECULES: HCl/Ar(111)

In this initial examination of the vibration–rotation spectrum of an adsorbed molecule, we have chosen our surface model to be a rectangular array of argon atoms fixed in their equilibrium lattice positions. This static surface composed of 24 atoms is then replicated in two dimensions via the imposition of periodic boundary conditions in order to describe the entire surface. We assume that the interaction of an HCl molecule with this surface can be described adequately by a sum of two-body potentials of the truncated Lennard-Jones form suggested by Weber and Stillinger,[22]

$$V_{ij} = A\epsilon_{ij}[(\sigma_{ij}/r_{ij})^{12} - 1]\exp\{(r_{ij}/\sigma_{ij} - a)^{-1}\},$$
$$0 < (r_{ij}/\sigma_{ij}) < a$$
$$= 0, \quad a \leqslant (r_{ij}/\sigma_{ij}),$$

where $A = 8.805\,977$, $a = 1.652\,194$, σ_{ij} and ϵ_{ij} are Lennard-Jones parameters for the interaction of one of the atoms of the molecule (i = H, Cl) with the jth Ar atom of the surface, and $r_{ij} = |\mathbf{r}_i - \mathbf{r}_j|$. The Lennard-Jones parameters chosen here are the same ones used by Diestler[23] in his model for HCl trapped in an Ar matrix, $\sigma_{H,Ar} = 3.1$ Å, $\epsilon_{H,Ar} = 67$ K, $\sigma_{Cl,Ar} = 3.4$ Å, $\epsilon_{Cl,Ar} = 90$ K. For a potential of this form, the equilibrium position of a physisorbed HCl molecule is such that the molecular bond axis lies almost parallel to the surface plane (with HCl at its equilibrium bond length, the average binding heights as revealed by a Monte Carlo random walk[24] are 3.39 ± 0.04 Å and 3.17 ± 0.05 Å for Cl and H, respectively). But in truth it is not at all clear just what the correct binding geometry should be for this system. We do know that experiments[25] have shown the van der Waals complex Ar–H–Cl to be linear with the indicated arrangement of the atoms, but these same experiments have also indicated that the complex undergoes large amplitude bending motions. Perhaps, therefore, the present model does represent at least a plausible description of the molecule–surface interaction.

While a single trajectory is sufficient for determining a pair of lines in the spectrum of an isolated molecule, an average of the intensity over a number of trajectories is required when examining an adsorbed molecule, since the spectrum obtained from one trajectory will depend on the initial position of the molecule with respect to the surface and the initial molecular center-of-mass velocity vector. The set of initial positions was obtained via a thermally biased random walk[24] at an assumed system temperature of 50 K. In this walk we constrained the motion of the molecule such that the bond length remained fixed at its equilibrium value and the angle between the bond axis and a plane parallel to the surface was a constant (10° as determined from the equilibrium binding heights given above). The components of the center-of-mass momentum vector were chosen at random from the appropriate Boltzmann distribution of velocities, while the momentum components deriving from vibrational and rotational motion were assigned in a like manner as for the free molecule. Note that the plane of the rotation of the adsorbed HCl molecule may be chosen either so as to give a particular projection of the angular momentum on the surface normal or at random. A comparison of the spectrum calculated for the $J = 0 \leftrightarrow 1$ transition on the basis of trajectories in which the initial projection of $\mathbf{L}$ onto the z axis was a maximum with a similar one obtained using random choices of the projection did not, however, reveal any noticeable differences between the two approaches.

In Fig. 2 one finds the result obtained from trajectories that in the absence of the interaction with the surface would yield the $R(0)$ and $P(1)$ lines of Fig. 1. Now instead of two

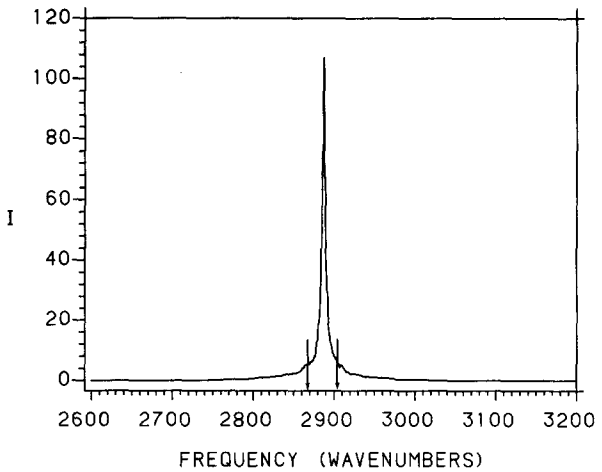

FIG. 2. Spectrum of adsorbed $^1H^{35}Cl$, $v_c = 1/2$ and $J_c = 1/2$. The arrows indicate the positions of the free molecule lines calculated using the same initial values of the action variables [$R(0)$ and $P(1)$].

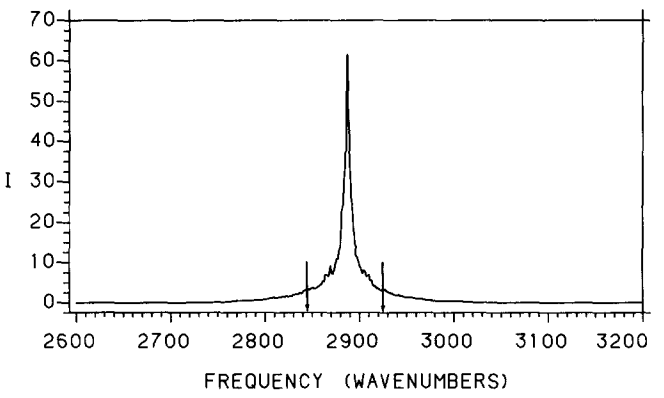

FIG. 3. Spectrum of adsorbed $^1H^{35}Cl$, $v_c = 1/2$ and $J_c = 3/2$. The arrows indicate the positions of the corresponding $R(1)$ and $P(2)$ lines.

lines, only a single line appears, centered about the frequency at which the Q branch would appear in the spectrum of the isolated molecule if the feature were allowed. The linewidth here clearly exceeds the resolution of the present calculations, with the broadening appearing to be homogeneous. (A summary of the information contained in this spectrum and in the spectra calculated at higher J_c values can be found in Table II.) At the base of the peak, near the positions of the free-molecule $R(0)$ and $P(1)$ peaks, there also seems to be a bit more intensity than might be expected from a continuation of the contour of the central peak into the wings. The line shape function as displayed in Fig. 2 was obtained on the basis of the results from 129 individual trajectories, although no significant difference is found when only 42 trajectories are included (i.e., the peak position, width, and integrated intensity are unchanged within the reported accuracy).

A similar sort of result is found when trajectories are begun with a rotational action variable, J_c, of 3/2 [corresponding to the transitions that yield the $R(1)$ and $P(2)$ lines in the isolated molecule]. However, while the total intensity under the peak shown in Fig. 3 differs negligibly from that calculated in the $J_c = 1/2$ case, the width here is substantially greater, with additional intensity being shifted into the wings. This trend continues when an additional unit of angular momentum is added ($J_c = 5/2$, Fig. 4)–a large fraction of the total line intensity has moved into the wings but no change in the integrated intensity has occurred. Note that the base of the peak is broadened to the extent that appreciable intensity can be found over a range of about 150 cm^{-1}. We doubt that any significance can be attached to the structure appearing in the wings of this peak, since it is very likely to be damped out as the number of trajectories included in the averaging is increased.

One, however, obtains a qualitatively different spectrum for an adsorbed HCl molecule initially excited to an even higher rotational state. The semiclassical simulation of the $(0,5) \rightarrow (1,6)$ and $(0,6) \rightarrow (1,5)$ transitions produces a spectrum composed of *three* lines, a weak line appearing at the fundamental frequency and two very broad features, one on either side of the band center (see Fig. 5). Clearly, this spectrum indicates that a transition between dynamical regimes is occurring as the rotational energy of the molecule increases, but at the particular energy considered here this new regime does not yet appear to involve free rotation, since the absorption features are found well away from the isolated molecule lines. Only at higher rotational energies can a free rotor picture be considered valid, an example of this situation being given in Fig. 6. The two peaks obtained from

TABLE II. Spectral lines for $^1H^{35}Cl/Ar(111)$

v_c	J_c	Number of trajectories[a]	Position $\tilde{\nu}$ (cm^{-1})	FWHM (cm^{-1})	$\bar{I}$ (D^2)
1/2	1/2	129 (130)	2887	4	4.93×10^{-3}
1/2	3/2	80 (80)	2887	6.5	4.85×10^{-3}
1/2	5/2	79 (81)	2887	7	4.90×10^{-3}
1/2	11/2	52 (390)	~2970	~55	3.97×10^{-3}
			2886	4	6.50×10^{-5}
			~2790	~70	4.82×10^{-3}
1/2	21/2	62 (81)	3080	5.5	2.22×10^{-3}
			2640	11	3.94×10^{-3}

[a] Only the nondesorbing trajectories are included in the intensity calculation. The number in parentheses is the total (desorbing and nondesorbing) number of trajectories run at the indicated (v_c, J_c).

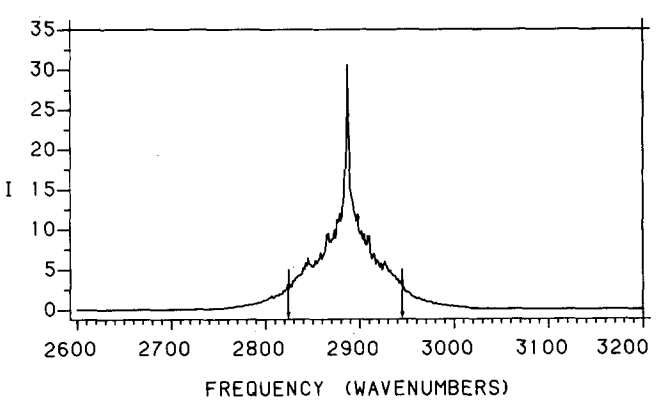

FIG. 4. Spectrum of adsorbed $^1H^{35}Cl$, $v_c = 1/2$ and $J_c = 5/2$. The arrows indicate the positions of the corresponding $R(2)$ and $P(3)$ lines.

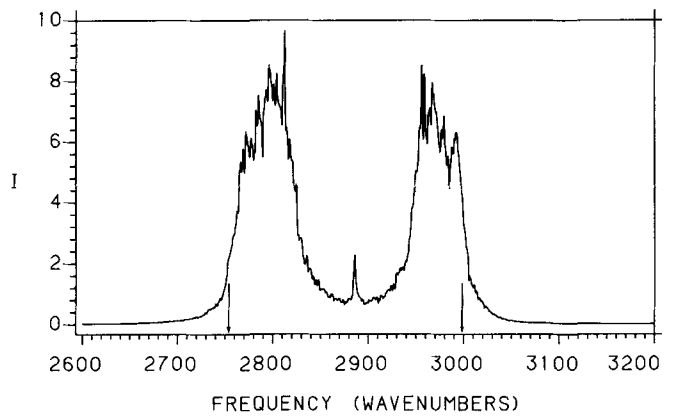

FIG. 5. Spectrum of adsorbed $^1H^{35}Cl$, $v_c = 1/2$ and $J_c = 11/2$. The arrows indicate the positions of the corresponding $R(5)$ and $P(6)$ lines.

$J_c = 21/2$ trajectories, while definitely broadened, are located essentially just where one would expect the $R(10)$ and $P(11)$ lines to arise.

There is an additional interesting result which is worth mentioning at this point, one not deriving from the spectra themselves. In performing the averages over individual trajectories, we include only the contributions from those trajectories that describe a molecule that remains bound to the surface for the entire 24.573 ps. At the lowest rotational energies very few trajectories lead to desorption over this time interval (for $J_c = 1/2$, 1 trajectory out of 130 is desorptive, while for $J_c = 3/2$ one finds that none of the 80 trajectories run here are desorptive), but the fraction desorbing increases markedly with increasing energy. For example, the highest rotational energy considered here, corresponding to $J_c = 21/2$, is associated with a 23% probability of desorption. It is the intermediate case, $J_c = 11/2$, that deserves special attention, however, for we find that 87% of these trajectories desorb during the indicated time span! In short, there seems to be evidence for an enhancement of the rate of desorption appearing in connection with the transition between the dynamical regimes that is suggested by the rotational energy dependence of the absorption line shape. Questions concerning the characterization of this particular type of rotationally enhanced desorption will be addressed in a future publication.

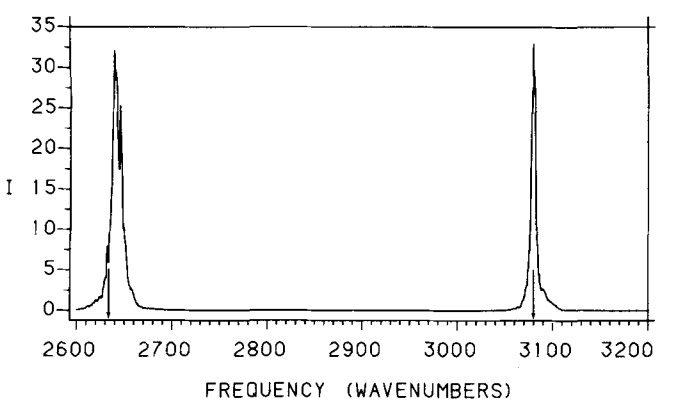

FIG. 6. Spectrum of adsorbed $^1H^{35}Cl$, $v_c = 1/2$ and $J_c = 21/2$. The arrows indicate the positions of the corresponding $R(10)$ and $P(11)$ lines.

V. ANALYSIS AND DISCUSSION

Given the previous success of the semiclassical spectral intensity method in predicting vibrational intensities in both model and real molecular systems, it should not be surprising that good results can also be obtained when rotation is included. Worth recalling, however, is our demonstration that the same simple correspondence principle which leads to an agreement between the quantum vibrational intensities and the ones deriving from classical trajectories[8] (namely, that the initial classical action variable should be an arithmetic average of quantum numbers labeling the initial and final states of the transition) applies equally well in the characterization of rotational state changes.[26] The method would thus be useful not only in studies of V → V intermolecular energy redistribution, but also in investigations of energy transfer which is enhanced as a consequence of the coupling of vibrational and rotational states. Our present interest in the results from the isolated molecule spectrum calculations stems principally, though, from the fact that they yield "standards" against which the spectra of dynamically more complex systems may be compared.

That a single mean-action trajectory will yield a pair of peaks, one in the R branch and the other in the P branch of the spectrum, can be easily understood if one considers a simple model problem. The classical motion of a harmonic oscillator/rigid rotor constrained to move in two dimensions is described by the expressions

$$\mathbf{r}(t) = r(t)\cos\omega_r t\hat{x} + r(t)\sin\omega_r t\hat{y},$$
$$r(t) = r_e + A\cos\omega_v t,$$

where $\mathbf{r}$ is the internal coordinate vector, ω_r and ω_v are the frequencies of the rotation and vibration, respectively, A is the amplitude of the vibration, and r_e is (as before) the equilibrium length of the oscillator/rotor. By combining these two equations and making use of simple trigonometric identities, one finds that

$$\mathbf{r}(t) = r_e\cos\omega_r t\hat{x} + r_e\sin\omega_r t\hat{y} + (A/2)[\cos(\omega_v+\omega_r)t\hat{x} + \sin(\omega_v+\omega_r)t\hat{y}] + (A/2)[\cos(\omega_v-\omega_r)t\hat{x} + \sin(\omega_v-\omega_r)t\hat{y}].$$

The structure of this result immediately suggests that a product of the form $\mathbf{r}(0)\cdot\mathbf{r}(t)$ will lead, when Fourier transformed, to a pure rotation line appearing at ω_r and a pair of vibration–rotation lines appearing at frequencies of $\omega_v + \omega_r$ and $\omega_v - \omega_r$ (with no "Q-branch" line at ω_v being observed). Since to first order $\mu(t) - \mu_0 \propto r(t) - r_e$, this model correctly predicts that a single trajectory should indeed yield the structure seen, for example, in Fig. 1. (An examination of the low-frequency end of one of our calculated free-molecule spectra does indeed reveal the presence of a pure rotation peak at the frequency predicted by the well-known quantum mechanical expression $\tilde{\nu} = hcB_eJ'$, where J' here is the quantum number of the upper rotational level involved in the transition. For molecules with rotation constants that are considerably smaller than B_e for HCl, an increase in the

resolution over that which is reported here clearly will be required if one is to obtain an accurate low-frequency spectrum.)

The more complicated system considered here, a diatomic molecule physisorbed on a rare gas crystal, clearly exhibits a transition between distinct dynamical regimes as the rotational energy of the molecule is increased. At the lowest energies the R- and P-branch structure of the fundamental absorption band collapses to a single peak appearing at the fundamental frequency, with this outcome indicating that trajectories with low rotational energies are characterized by zero average angular momentum ($\langle \mathbf{L} \rangle = 0$). But in addition to the collapse of structure, a peak broadening is also observed that cannot, since the crystal surface is taken to be static in the current model, be attributed to coupling with surface phonons. Nor is it likely that V $\leftrightarrow$ R intermolecular energy transfer plays a very significant role in the broadening mechanism, since the frequency mismatch between the two modes is quite large. A much more reasonable explanation for the broadening lies, therefore, in a loss of rotational phase coherence as a consequence of frequent collisions with the surface, particularly those involving collisions of the lighter and less tightly bound hydrogen atom. A detailed examination of such a trajectory indeed bears out this analysis—while the chlorine atom executes diffusive motion across the surface, the hydrogen atom undergoes frequent changes of direction in all three dimensions. With an increase in the rotational energy, which is manifested primarily as an increase in the velocity of the hydrogen atom, one would thus expect to find an acceleration of this dephasing and an increase in the widths of the higher J_c lines, a result that is indeed observed in our spectra. We note that a pure dephasing mechanism has also been proposed by Tully *et al.*,[12] as an explanation of the temperature dependence of the vibrational linewidths measured for a hydrogen overlayer on a Si(100) surface. In addition, the destruction of rotational phase coherence has been observed in several related studies. Polanyi and Wolf,[27] in their investigation of a diatomic molecule impinging on a smooth solid surface, identified a number of trajectories involving a change in the sign of the molecular angular momentum ("chattering" trajectories) both when the scattering was direct and when there was a significant degree of rotational trapping. Similar calculations by Bowman and Park[28] of rotational excitation in rigid rotor–rigid surface scattering also have suggested that rotational dephasing processes constitute an important feature of microscopic molecule–surface collision dynamics.

From the calculated linewidth, a rotational dephasing lifetime can be extracted that should give us a feel for just how significant is the perturbation of molecular rotation by the solid surface. Consider first the $J_c = 1/2$ case, for which the FWHM is estimated to be 4 cm^{-1}. This width suggests a value of $\sim$0.8 ps for the lifetime of the coherent state, which when compared with the rotational period of the free molecule with the same initial angular momentum (1.82 ps) indicates that dephasing occurs within $\sim$0.4–0.5 of a rotational period. This result alone would lead us to conclude that rotation is strongly affected by the gas–surface interaction, even in the absence of the corroborating examination of the trajectories themselves. One can also easily demonstrate that the width of the $J_c = 3/2$ line is likewise consistent with a loss of rotational phase coherence within about half of a rotation.

In the high rotational energy regime the analysis of the spectrum appears to be straightforward. The fact that the absorption peaks of the adsorbed molecule (more or less) overlap those of the free molecule implies that the bound molecule can be thought of as a free rotor, whose motion is only slightly perturbed (as evidenced by the presence of some line broadening) by the interaction with the surface. We would therefore predict that if discrete structure is to be observed in the experimental spectrum of a physisorbed diatomic, it will most likely be found in the high-J wings of the fundamental band rather than near the central frequency.

An experimental spectrum represents, of course, a superposition of the individual spectra obtained in the present work, with each contribution appropriately Boltzmann weighted. Consequently, if many rotational states are significantly populated at the given system temperature, the broad central feature of the spectrum will be comprised of several peaks, each with its own characteristic width. Deduction of lifetimes even for purely elastic processes from an analysis of the width of the resulting spectral feature will therefore be suspect, unless some sort of deconvolution can be performed. By going to lower temperatures one can minimize this problem, since then fewer rotational states will contribute, but it may or may not be possible to make conclusions about the dynamics at the higher temperature on the basis of the low temperature measurements. We feel, though, that theoretical studies of the sort presented here will provide a useful means for analyzing this experimental data through the simulation of spectra in much the same way that normal mode calculations have elucidated the structure and dynamics of gaseous species.

In order to confirm the dynamical conclusions drawn from the calculated spectra, we have extracted from the trajectories the time dependence of the two HCl orientation angles, θ and ϕ. (The θ angle describes the orientation of the molecular axis with respect to a line normal to the surface,

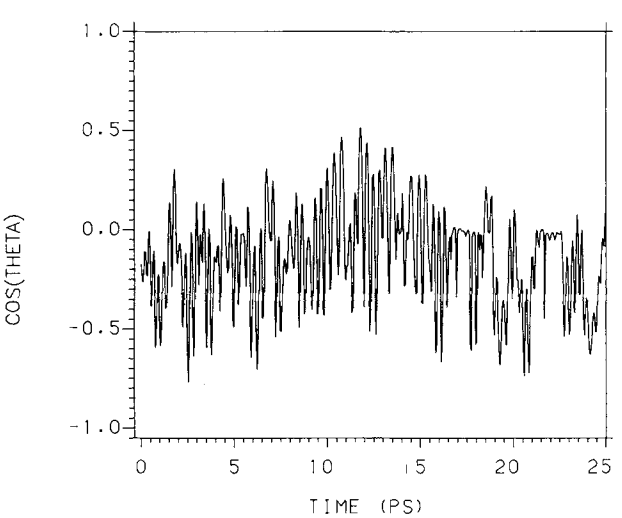

FIG. 7. Cos $\theta(t)$ for an HCl/Ar trajectory corresponding to the $v = 0 \rightarrow 1$, $J = 0 \leftrightarrow 1$ spectral transitions (i.e., $v_c = 1/2$, $J_c = 1/2$).

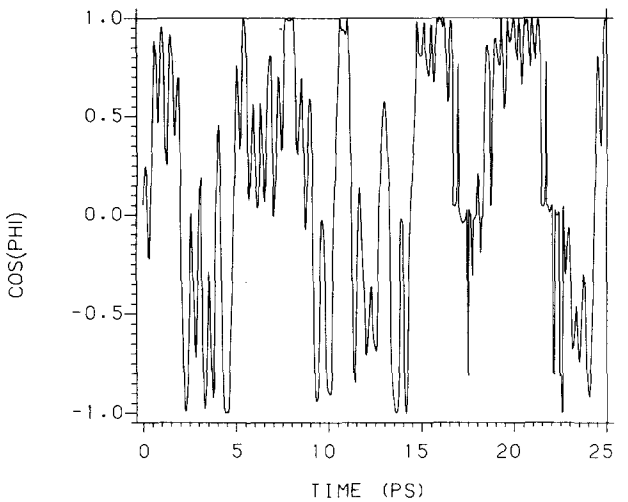

FIG. 8. Cos $\phi(t)$ for the same trajectory as in Fig. 7.

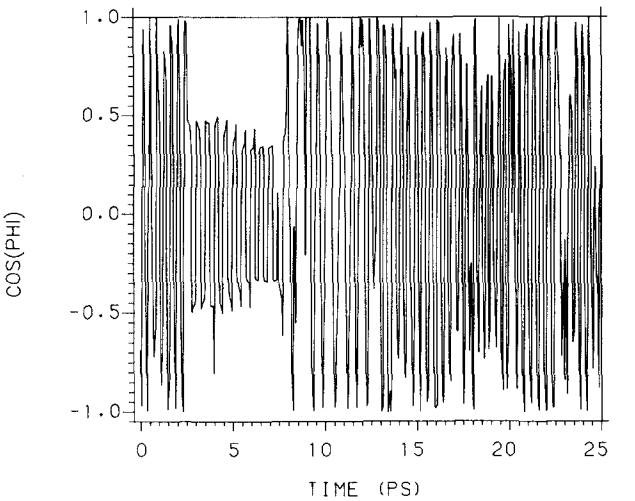

FIG. 10. Cos $\phi(t)$ for the same trajectory as in Fig. 9.

such that if the molecule lies perpendicular to the surface plane with the chlorine atom closest to the argon, then $\theta = 0$. On the other hand, ϕ is measured in a plane parallel to the surface layer and passing through the molecule's center of mass. The projection onto this plane of a vector extending from the center of mass to the hydrogen atom makes an angle ϕ with a second vector that extends from the center of mass in the $[\bar{1}10]$ surface direction.) We begin with an example of a trajectory describing the $v = 0 \rightarrow 1$, $J = 0 \leftrightarrow 1$ transitions. In Figs. 7 and 8 one finds plots of cos θ and cos ϕ, respectively, vs time, and one concludes that the hindered rotation model suggested above indeed does reflect well the observed microscopic molecular dynamics. While the value of θ oscillates over a range of about 60° with the average value appearing to be somewhat greater than 90° (with 90° corresponding to HCl lying parallel to the surface—note that the equilibrium HCl binding geometry mentioned in Sec. IV leads to a value for θ of 100° and thus a value for cos θ of -0.17), ϕ clearly takes on the entire range of its possible values. Figure 8 indicates that in this trajectory there is an overall periodic variation in ϕ occurring on a 3–5 ps time scale upon which a higher frequency oscillatory behavior having a period of 0.5–1 ps is superimposed. This latter period compares well with the 0.8 ps rotational dephasing time estimated from the width of the calculated spectral peak.

The dynamical picture which emerges from the trajectories describing the intermediate J transitions differs greatly from this hindered rotor model, however. In Figs. 9 and 10 we display the time variation in the angles for a characteristic $J = 5 \leftrightarrow 6$ trajectory and note that in this regime the molecule appears to be tumbling wildly. Both θ and ϕ pass through their entire range of values with a period which is $\leqslant 0.5$ ps. Recall that we have also reported a high probability of desorption of these molecules during the 25 ps trajectory integration time, with this result being quite consistent with the free tumbling dynamics indicated by these angle plots.

Higher degrees of rotational excitation are associated with yet another sort of molecular motion, as we clearly can see from Figs. 11 and 12. The first of these plots, showing the time dependence of θ, is actually very similar to Fig. 7, except that the frequency of oscillation is now higher. Thus at the higher angular momentum values, the molecule again

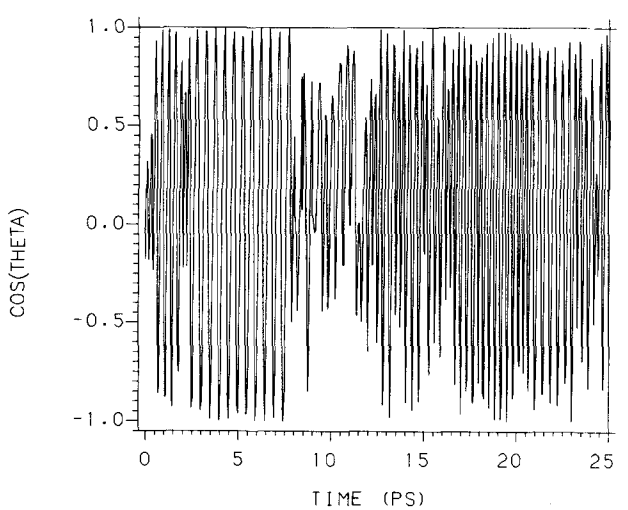

FIG. 9. Cos $\theta(t)$ for an HCl/Ar trajectory corresponding to the $v = 0 \rightarrow 1$, $J = 5 \leftrightarrow 6$ spectral transitions.

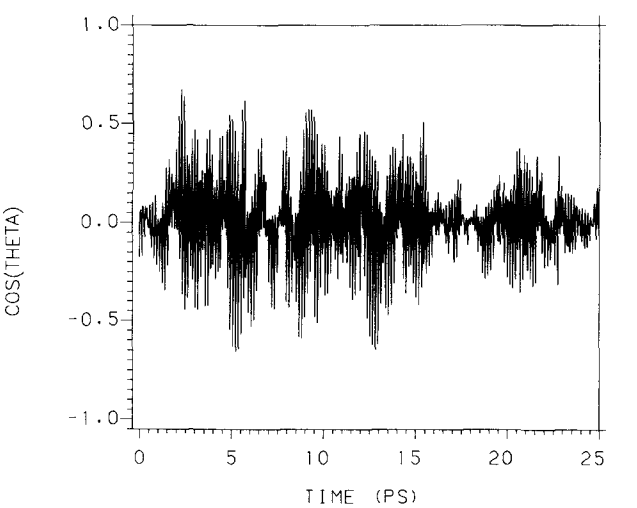

FIG. 11. Cos $\theta(t)$ for an HCl/Ar trajectory corresponding to the $v = 0 \rightarrow 1$, $J = 10 \leftrightarrow 11$ spectral transitions.

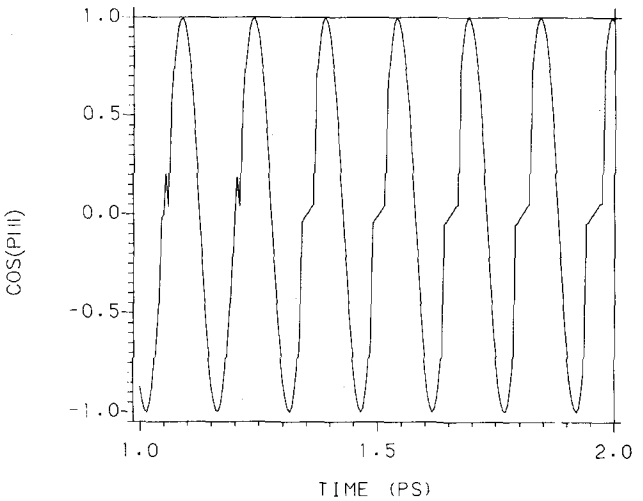

FIG. 12. Cos $\phi(t)$ for the same trajectory as in Fig. 11.

chiefly rotates in a plane parallel to the surface. Note that here the average value of θ for the displayed trajectory is seen to be essentially zero, so that the rotating molecule lies, on the average, with the chlorine and hydrogen atoms equidistant from the surface. Figure 12 indicates, though, that the molecule is (almost) freely rotating about the surface normal. (Only a segment of the cos ϕ plot is shown here since an expanded time scale is required if the structure is to be resolved.) Although some perturbation of the periodic structure is evident here (and, consequently, our calculated spectral lines are not infinitely narrow) we are led to conclude that only a small error will be introduced by treating the molecule as a free rotor in this regime. Actually, the high J_c value trajectories are quite similar to those obtained at the lowest J_c's, except that the rapidly rotating molecules are not as strongly affected by the local variations in the molecule–surface potential. The transition from hindered rotation to free rotation by no means occurs smoothly, however, as we have seen from the results displayed in Figs. 5, 9, and 10.

In summary, we have shown that by using the semiclassical spectral intensity method of Marcus and co-workers one can obtain not only vibration–rotation spectra in which the individual R and P lines are resolved (in contrast to the purely classical calculation of Berens and Wilson[10] that yields only the envelope of the absorption) but also the analogous spectra of species physisorbed on a solid surface. Of particular importance in the present work is the identification of distinct dynamical limits characterizing the motion of the adsorbed diatomic, the transition from one to the other occurring as the rotational energy is increased. In addition it appears that a purely elastic process, rotational dephasing, gives rise to the line broadening observed in the simulated spectra. Overall we feel that the current formalism provides a quite attractive approach to the study of the structure and dynamics of adsorbed species, one that will aid significantly in the interpretation of experimental data.

ACKNOWLEDGMENTS

The author wishes to thank the Research Council of the University of Missouri–Columbia for a Summer Research Fellowship in support of this work and also R. M. Stratt for useful discussions in connection with the research. In addition, the helpful comments of the referee concerning the interpretation of the results are gratefully acknowledged.

[1]See, for example, *Vibrational Intensities in Infrared and Raman Spectroscopy*, edited by W. B. Person and G. Zerbi (Elsevier, Amsterdam, 1982).
[2]See, for example, M. L. Hair, *Infrared Spectroscopy in Surface Chemistry* (Dekker, New York, 1967).
[3]Examples of recent work are found in *Vibrational Spectroscopy of Adsorbates*, edited by R. F. Willis (Springer, Berlin, 1980); *Vibrational Spectroscopies for Adsorbed Species*, ACS Symp. Ser. No. 137, edited by A. T. Bell and M. L. Hair (American Chemical Society, Washington, D. C., 1980).
[4]S. Chiang, R. G. Tobin, P. L. Richards, and P. A. Thiel, Phys. Rev. Lett. **52**, 648 (1984).
[5]Y. J. Chabal, G. S. Higashi, and S. B. Christman, Phys. Rev. B **28**, 4472 (1983).
[6]D. W. Noid, M. L. Koszykowski, and R. A. Marcus, J. Chem. Phys. **67**, 404 (1977).
[7]M. L. Koszykowski, D. W. Noid, and R. A. Marcus, J. Phys. Chem. **86**, 2113 (1982).
[8]D. M. Wardlaw, D. W. Noid, and R. A. Marcus, J. Phys. Chem. **88**, 536 (1984).
[9]J. R. Stine and D. W. Noid, J. Chem. Phys. **78**, 1876 (1983).
[10]P. H. Berens and K. R. Wilson, J. Chem. Phys. **74**, 4872 (1981). An extension has also been made to Raman spectroscopy. See P. H. Berens, S. R. White, and K. R. Wilson, *ibid.* **75**, 515 (1981). *Ab initio* infrared and Raman spectra are reported in D. R. Fredkin, A. Komornicki, S. R. White, and K. R. Wilson, *ibid.* **78**, 7077 (1983).
[11]J. R. Reimers and R. O. Watts, Chem. Phys. **85**, 83 (1984).
[12]J. C. Tully, Y. J. Chabal, K. Raghavachari, J. M. Bowman, and R. R. Lucchese, Phys. Rev. B **31**, 1184 (1985).
[13]R. G. Gordon, Adv. Magn. Reson. **3**, 1 (1968). D. A. McQuarrie, *Statistical Mechanics* (Harper and Row, New York, 1976), Chap. 21.
[14]A. Papoulis, *Probability, Random Variables, and Stochastic Processes* (McGraw-Hill, New York, 1965), pp. 336–352.
[15]P. F. Naccache, J. Phys. B **5**, 1308 (1972).
[16]H. Nichols and R. M. Hexter, J. Chem. Phys. **73**, 965 (1980).
[17]G. Herzberg, *Spectra of Diatomic Molecules* (Van Nostrand, New York, 1950), p. 534.
[18]R. H. Tipping and J. F. Ogilvie, J. Mol. Struct. **35**, 1 (1976).
[19]J. F. Ogilvie, W. R. Rodwell, and R. H. Tipping, J. Chem. Phys. **73**, 5221 (1980).
[20]See, for example, R. N. Porter and L. M. Raff, in *Dynamics of Molecular Collisions; Part B*, edited by W. H. Miller (Plenum, New York, 1976). An expression for the energy levels of a Dunham-type oscillator in terms of the action variable is given by W. H. Miller, Adv. Chem. Phys. **25**, 69 (1974).
[21]N. L. Alpert, W. E. Keiser, and H. A. Szymanski, *IR, Theory and Practice of Infrared Spectroscopy*, 2nd ed. (Plenum, New York, 1970), Fig. 4-1B.
[22]T. A. Weber and F. H. Stillinger, J. Chem. Phys. **80**, 2742 (1984).
[23]D. J. Diestler, J. Chem. Phys. **78**, 2240 (1983).
[24]J. P. Valleau and S. G. Whittington, in *Statistical Mechanics*; Part A, edited by B. J. Berne (Plenum, New York, 1977).
[25]S. E. Novick, P. Davies, S. J. Harris, and W. Klemperer, J. Chem. Phys. **59**, 2273 (1973); S. E. Novick, K. C. Janda, S. L. Holmgren, M. Waldman, and W. Klemperer, *ibid.* **65**, 1114 (1976).
[26]The good agreement between the present semiclassical vibration–rotation spectra and the corresponding experimental results (i.e., the "quantum mechanical" spectra) is not expected to persist if the classical dynamics is followed for arbitrarily long times. As demonstrated by Berne, the classical dipolar autocorrelation function, while identical with the analogous quantum result for short times, lacks the recurrence behavior characteristic of the quantum rotor. The calculations reported here, however, do not involve trajectories that are of a sufficient length for there to be an appreciable difference in the behavior of the classical and quantum systems. See B. J. Berne, in *Physical Chemistry, An Advanced Treatise*, edited by H. Eyring, D. Henderson, and W. Jost (Academic, New York, 1971), Vol. VIIIB, pp. 682–689.
[27]J. C. Polanyi and R. J. Wolf, Ber. Bunsenges. Phys. Chem. **86**, 356 (1982).
[28]J. M. Bowman and S. C. Park, J. Chem. Phys. **77**, 5441 (1982); S. C. Park and J. M. Bowman, *ibid.* **80**, 2183 (1984).